Head-to-Head Cross-Linked Adduct between the Antitumor Unit Bis(μ-N,N′-di-p-tolylformamidinato)dirhodium(II,II) and the DNA Fragment d(GpG)

ARTICLE *in* CHEMISTRY · AUGUST 2006

Impact Factor: 5.73 · DOI: 10.1002/chem.200600401 · Source: PubMed

2 AUTHORS, INCLUDING:

Kim R Dunbar
Texas A&M University
442 PUBLICATIONS **13,187** CITATIONS

SEE PROFILE

DOI: 10.1002/chem.200600401

Dirhodium(II,II) DNA Head-to-Head Cross-Links

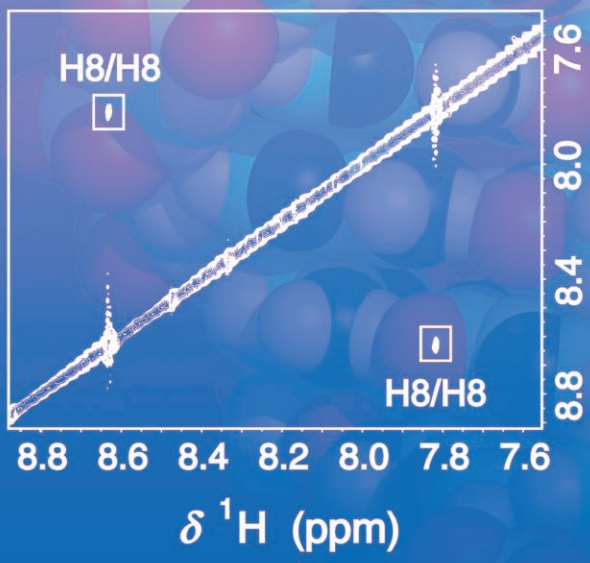

ROESY NMR

$[Rh_2(DTolF)_2\{d(GpG)\}]$

$[Rh_2(O_2CCH_3)_2\{d(GpG)\}]$

Head-to-Head Cross-Linked Adduct between the Antitumor Unit Bis(μ-*N,N′*-di-*p*-tolylformamidinato)dirhodium(II,II) and the DNA Fragment d(GpG)

Helen T. Chifotides* and Kim R. Dunbar*[a]

Abstract: Reactions of the compound *cis*-$[Rh_2(DTolF)_2(CH_3CN)_6](BF_4)_2$, a formamidinate derivative of the class of antitumor compounds $[Rh_2(O_2CR)_4]$ (R = Me, Et, Pr), with 9-ethylguanine (9-EtGuaH) or the dinucleotide d(GpG) proceed by substitution of the acetonitrile groups, with the guanine bases spanning the Rh–Rh bond, in a bridging fashion, through sites *N7/O6*. In the case of 9-EtGuaH, both head-to-head (HH) and head-to-tail (HT) isomers are formed, whereas with the tethered bases in d(GpG), only *one right-handed* conformer HH1R $[Rh_2(DTolF)_2\{d(GpG)\}]$ is present in solution. For both *cis*-$[Rh_2(DTolF)_2(9\text{-}EtGuaH)_2](BF_4)_2$ and $[Rh_2(DTolF)_2\{d(GpG)\}]$, the absence of *N7* protonation at low pH and the substantial decrease of the pK_a values for *N1-H* deprotonation, support *N7/O6* binding of the bases to the dirhodium core. The *N7/O6* binding of the bases is further corroborated by the downfield shift by $\Delta\delta \sim 4.0$ ppm of the ^{13}C NMR resonances for the C6 nuclei as compared to the corresponding resonances of the free ligands. The HH arrangement of the guanine bases in $[Rh_2(DTolF)_2\{d(GpG)\}]$ is indicated by the intense H8/H8 ROE cross-peaks in the 2D ROESY NMR spectrum. Complete characterization of the $[Rh_2(DTolF)_2\{d(GpG)\}]$ conformer by 2D NMR spectroscopy supports *anti*-orientation and N (C3′-*endo*) conformation for both deoxyribose residues. The N-pucker for the 5′-G base is universal in such cross-links, but it is very unusual for platinum and unprecedented for dirhodium HH cross-linked adducts to have both deoxyribose residues in the N-type conformation. The bulk, the nonlabile character, and the electron-donating ability of the formamidinate bridging groups spanning the dirhodium core affect the nature of the preferred dirhodium DNA adducts. Molecular modeling studies performed on $[Rh_2(DTolF)_2\{d(GpG)\}]$ corroborate the structural features obtained by NMR spectroscopy.

Keywords: nucleic acids · antitumor agents · bioinorganic chemistry · formamidinates · N ligands · rhodium

Introduction

Metal–metal-bonded dirhodium compounds[1] with a lantern type structure have attracted scientific interest due to their appreciable carcinostatic activity against various tumor cell lines. Pioneering studies that emanated in the 1970s revealed that dirhodium tetracarboxylate compounds of the type $[Rh_2(O_2CR)_4]$ (R = Me, Et, Pr; Scheme 1a) exhibit significant in vivo antitumor activity against L1210 tumors,[2,3] Ehrlich ascites,[4–7] as well as sarcoma 180 and P388 tumor lines.[8] Although the exact mechanism of their antitumor activity has not yet been elucidated, previous studies support the conclusions that dirhodium compounds bind to DNA,[4,5,9–12] and inhibit DNA replication, protein synthesis, and in vitro transcription.[13–16]

Another closely related class of dirhodium compounds to the tetracarboxylate series has emerged by substituting the carboxylate for the more robust amidinate groups.[1] Despite the lack of any appreciable biological activity of the homoleptic paddlewheel compound $[Rh_2(DTolF)_4]$ (DTolF = anion of *N,N′*-di-*p*-tolylformamidinate) due to steric factors,[17] the compound *cis*-$[Rh_2(DTolF)_2(O_2CCF_3)_2(H_2O)_2]$ (Scheme 1b) exhibits antitumor activity comparable to that of the dirhodium carboxylates and cisplatin (when supplied in the same quantity) against Yoshida ascites and T8 sarcomas with considerably reduced toxicity.[18] The two labile trifluoroacetate bridging groups impart an appreciable reactivity to the complex, yet its toxic side effects are minimal. It is

[a] Dr. H. T. Chifotides, Prof. K. R. Dunbar
Department of Chemistry, Texas A&M University, College Station, TX 77843 (USA)
Fax: (+1) 979-845-7177
E-mail: dunbar@mail.chem.tamu.edu
chifotides@mail.chem.tamu.de

Supporting information for this article is available on the WWW under http://www.chemeurj.org/ or from the author.

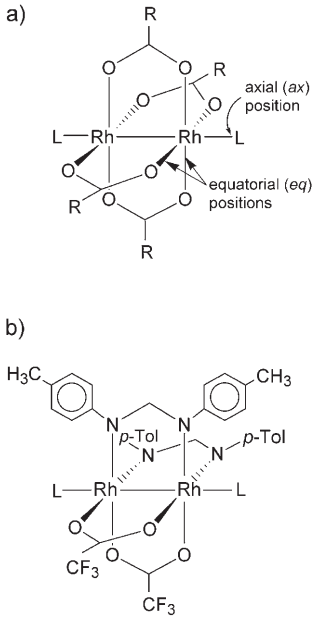

Scheme 1. Structures of metal–metal-bonded dirhodium compounds.

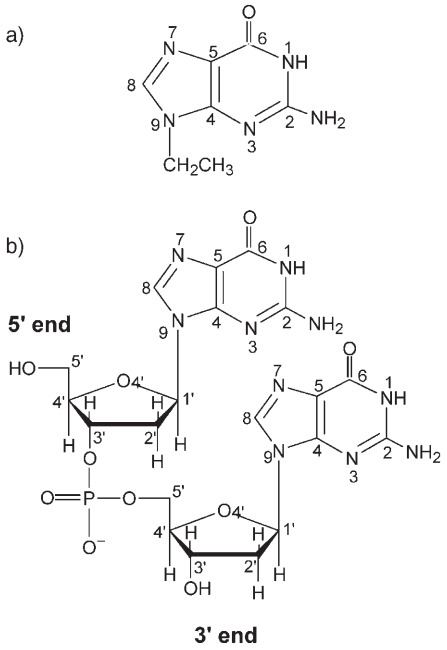

Scheme 2. Structure and atom numbering of a) nucleobase 9-ethylguanine (9-EtGuaH) and b) dinucleotide d(GpG).

notable that it was not possible to establish the highest nontoxic dose for *cis*-$[Rh_2(DTolF)_2(O_2CCF_3)_2(H_2O)_2]$, since it would need to be dissolved in a volume of solvent (dimethyl sulfoxide) that would itself become toxic before the compound would be cytotoxic.[18]

In light of DNA being the primary target of most metal-based anticancer agents, the reactions of dirhodium compounds with purine nucleobases, nucleos(t)ides, single-[9,10] and double-stranded DNA[11] have received considerable attention.[12] Early claims in the literature that dirhodium carboxylate compounds do not react with guanine (Scheme 2a) and polyguanylic acids[4] were unequivocally settled by findings in our laboratories that guanine bases bind to the dirhodium core in a manner involving unprecedented equatorial (*eq*) bridging interactions. In particular, the crystal structural determinations of HT *cis*-$[Rh_2(O_2CCH_3)_2(9\text{-EtGua})_2(MeOH)_2]$,[19] HH *cis*-$[Rh_2(O_2CCH_3)_2(9\text{-EtGuaH})_2(Me_2CO)(H_2O)](BF_4)_2$[20] and HT *cis*-$[Rh_2(O_2CCF_3)_2(9\text{-EtGuaH})_2(Me_2CO)_2](CF_3CO_2)_2$,[19] revealed that bridging 9-EtGuaH groups (Scheme 2a) span the dirhodium unit through the *N7/O6* sites in a *cis* disposition and HH or HT orientations.[21] Notable features of HT *cis*-$[Rh_2(O_2CCH_3)_2(9\text{-EtGua})_2(MeOH)_2]$ are the deprotonation of the purine site *N1*, that is, stabilization of the enolate form of guanine (9-EtGua$^-$), and the substantial increase in the acidity of *N1-H* due to bidentate *N7/O6* coordination (pH dependent ^{1}H and ^{13}C NMR titrations afford a pK_a value of ~5.7 compared to 8.5 for *N7*-bound only and 9.5 for the unbound purine).[22] In the same vein, reactions of *cis*-$[Rh_2(DTolF)_2(O_2CCF_3)_2]$ or *cis*-$[Rh_2(DTolF)_2(CH_3CN)_6](BF_4)_2$ with 9-EtGuaH proceed by substitution of the carboxylate or acetonitrile groups, respectively, and afford adducts with both possible base orientations (HH and HT).[23] In particular, the single-crystal X-ray crystallographic determination of HH *cis*-$[Rh_2(DTolF)_2(9\text{-EtGuaH})_2(NCCH_3)](BF_4)_2$ revealed bridging 9-EtGuaH groups binding to equatorial sites of the dirhodium unit through *N7/O6*.[23] Related studies involving the reactions of *cis*-$[Rh_2(DTolF)_2(CH_3CN)_6](BF_4)_2$ with N–N chelates, which mimic the binding of two adjacent DNA bases (2,2′-bipyridine and 1,10-phenanthroline), demonstrated that the latter bind to the dirhodium core in a chelating fashion by substituting acetonitrile molecules in equatorial positions.[24]

Armed with the knowledge obtained from our studies of the dirhodium unit interactions with the basic building blocks of DNA, we extended our work to the chemistry of small DNA fragments. Reactions of $[Rh_2(O_2CCH_3)_4]$ with the dinucleotides d(GpG) (Scheme 2b) and d(pGpG) afford $[Rh_2(O_2CCH_3)_2\{d(GpG)\}]$[22] and $[Rh_2(O_2CCH_3)_2\{d(pGpG)\}]$,[25] respectively, with bidentate *N7/O6* bridging bases spanning the Rh–Rh bond. The bidentate *N7/O6* coordination of the bases is corroborated by the notable increase in the acidity of *N1-H* and the substantial downfield shifts of the ^{13}C NMR resonances of the base C6 carbon atoms.[22,25] For both dinucleotide complexes, intense H8/H8 ROE (Rotating frame nuclear Overhauser effect) cross-peaks in the 2D ROESY NMR spectra indicate a HH arrangement of the tethered guanine bases.[22,25] The $[Rh_2(O_2CCH_3)_2\{d(GpG)\}]$ complex exhibits two major *right*-handed conformers HH1R (~75%) and HH2R (~25%).[22] The terms HH1R and HH2R, initially proposed for platinum compounds by Kozelka et al.,[26,27] and refined by Marzilli et al.,[28–31] refer to the relative base canting and the direction of propagation of the phosphodiester backbone with respect to the 5′ base (Scheme 3).[22] HH1L platinum ad-

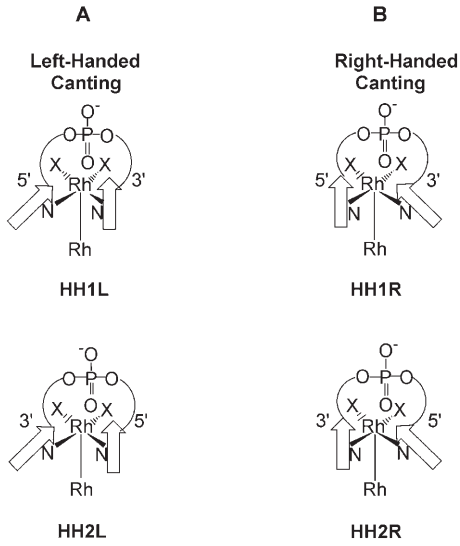

Scheme 3. Possible head-to-head (HH) variants of dirhodium-d(GpG) adducts with left- and right-handed canting. Canting arises from the fact that the G bases are not oriented exactly perpendicular to the N7-Rh-N7 plane. A) Left-handed (L) models and B) right-handed models (R); 1 and 2 refer to models with 5′-G and 3′-G positioned to the left, respectively. In parts A and B, the two rhodium atoms are considered as face-to-face square planes with the Rh atom attached to the N7 atoms depicted on the top and the X atoms of the attached bridging groups in the back; for the sake of clarity, the coordination sites for the second Rh atom are not shown. The G base is indicated with an arrow having H8 at the tip.

ducts with d(GpG) appear to dominate in solution, except for three reported cases.[28,30,32] The HH2 variants of d(GpG) adducts, however, have been elusive due to the degree of rotational freedom in cisplatin; they were first identified by Marzilli et al. by invoking retro models with carrier ligands (e.g., 2,2′-bipiperidine) on the platinum center that decrease the fluxional motion above and below the conformational plane.[28–31,33] In the case of the $[Rh_2(O_2CCH_3)_2\{d(GpG)\}]$ adducts, the unusual HHR conformers were most likely observed because of the combined effects of restricted rotation of the guanine about the Rh–N7 bond due to the bidentate *N7/O6* binding, and the presence of the acetate bridging groups.[22]

Detailed characterization of the HH1R and HH2R $[Rh_2(O_2CCH_3)_2\{d(GpG)\}]$ conformers by 2D NMR spectroscopy,[22] revealed notable structural features that resemble those of *cis*-$[Pt(NH_3)_2\{d(GpG)\}]$; the latter involve repuckering of the 5′-G sugar rings to the C3′-*endo* (N-type) conformation, retention of the C2′-*endo* (S-type) conformation for the 3′-G sugar rings and *anti*-orientation of the bases with respect to the glycosyl bonds.[22,25] Herein, we report the structural characterization of the biologically relevant adduct $[Rh_2(DTolF)_2\{d(GpG)\}]$ by one- (1D) and two-dimensional (2D) NMR spectroscopy along with molecular modeling studies. The conformational and structural characteristics of $[Rh_2(DTolF)_2\{d(GpG)\}]$ are discussed in light of the conferred effects of substituting the acetate for the formamidinate bridging groups on the dirhodium core.

Results

1D ^{1}H NMR spectroscopy

***cis*-$[Rh_2(DTolF)_2(9\text{-}EtGuaH)_2](BF_4)_2$**: The ^{1}H NMR spectrum of $[Rh_2(DTolF)_2(9\text{-}EtGuaH)_2](BF_4)_2$ in CD_3CN displays two H8 resonances in the aromatic region at $\delta = 8.05$ and 8.08 ppm, downfield from the H8 resonance of free 9-EtGuaH at $\delta = 7.49$ ppm (in CD_3CN). The two H8 resonances are attributed to the two isomers (HH and HT) of *cis*-$[Rh_2(DTolF)_2(9\text{-}EtGuaH)_2](BF_4)_2$ produced from the reaction of *cis*-$[Rh_2(DTolF)_2(NCCH_3)_6](BF_4)_2$ with 9-EtGuaH. In the same region, there are two triplets at $\delta = 7.41$ and 7.54 ppm, which are ascribed to the sets of N-C*H*-N groups of the bridging formamidinate groups for each isomer (the triplets are attributed to ^{1}H coupling to the two equivalent rhodium nuclei, $^3J\{^{103}Rh,^1H\} = 3.8$ Hz (for *cis*-$[Rh_2(DTolF)_2(NCCH_3)_6](BF_4)_2$, δ(N-C*H*-N) = 7.51 ppm in CD_3CN).

To study the behavior of the H8 protons of $[Rh_2(DTolF)_2(9\text{-}EtGuaH)_2](BF_4)_2$, a pH-dependence ^{1}H NMR titration was performed in CD_3CN (Figure 1). The pH-independent

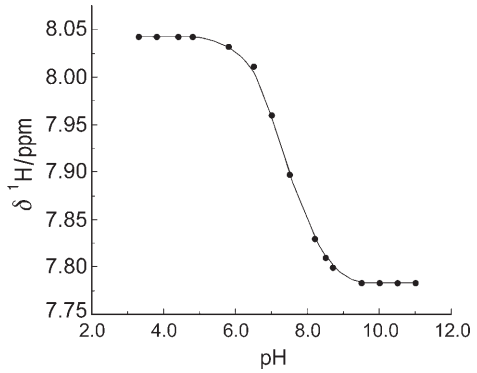

Figure 1. pH dependence of the H8 ^{1}H NMR resonance for $[Rh_2(DTolF)_2(9\text{-}EtGuaH)_2](BF_4)_2$ in CD_3CN at 20 °C. At each pH value, the ^{1}H NMR chemical shifts of the two $[Rh_2(DTolF)_2(9\text{-}EtGuaH)_2](BF_4)_2$ isomers differ by about 0.05 ppm, thus the titration curve for the second isomer has been omitted from the plot.

behavior of the H8 ^{1}H NMR resonance at low pH corroborates *N7* binding to the rhodium center (the bound metal prevents protonation of this site). For free 9-EtGuaH in D_2O, protonation of *N7* and (de)protonation of *N1* take place at pK_a ~2.5 and pK_a ~9.5, respectively.[22] For $[Rh_2(DTolF)_2(9\text{-}EtGuaH)_2](BF_4)_2$, the (de)protonation of *N1* takes place at pK_a ~7.3 in CD_3CN (Figure 1).

Owing to the very low solubility of 9-EtGuaH in CH_3CN, it was not possible to perform a pH-dependence titration of its H8 proton in CD_3CN. It has been demonstrated, however, that the pK_a values of neutral acids (and their conjugated bases) increase in organic solvents as compared to water (the decrease in the dielectric constant of the medium disfavors dissociation of neutral acids because it produces charged species, thus it increases the pK_a values;[34] for example, the pK_a of acetic acid is 4.76 and 22.3 in H_2O and CH_3CN, respectively).[35] It is thus inferred that the pK_a of 9-EtGuaH

in CD_3CN should be considerably higher than 9.5 (i.e., the pK_a of benzylamine is 9.33 and 16.8 in H_2O and CH_3CN, respectively).[35] Therefore, the pK_a value (~7.3) for $[Rh_2(DTolF)_2(9\text{-}EtGuaH)_2](BF_4)_2$ in CD_3CN has decreased considerably compared to free 9-EtGuaH. The substantial increase in the acidity of *N1-H* is attributed to the bidentate *N7/O6* binding to the dirhodium unit, a fact confirmed by the X-ray crystal structure of HH *cis*-$[Rh_2(DTolF)_2(9\text{-}EtGuaH)_2(NCCH_3)](BF_4)_2$[23] (the *N1*-H sites are not deprotonated in the crystal structure as in the acetate adduct HT *cis*-$[Rh_2(O_2CCH_3)_2(9\text{-}EtGua)_2(MeOH)_2]$,[19] presumably because CH_3CN does not need to be protonated to become a good leaving group).

$[Rh_2(DTolF)_2\{d(GpG)\}]$: In the aromatic region of the ^{1}H NMR spectrum of the dirhodium adduct in CD_3CN/D_2O 80/20% at 20°C, the two inequivalent nonexchangeable H8 protons of d(GpG) give rise to two resonances at $\delta = 8.73$ and 7.84 ppm (Figure 2; Table 1). These downfield and upfield resonances are assigned to the 5′-G and 3′-G H8 protons, respectively, by analysis of 2D NMR spectroscopic data (vide infra).

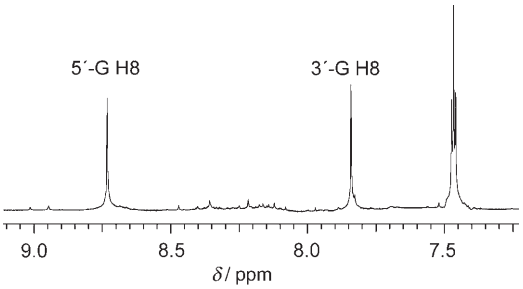

Figure 2. Aromatic region of the 1D ^{1}H NMR spectrum of $[Rh_2(DTolF)_2\{d(GpG)\}]$ in CD_3CN/D_2O 80/20% at 20°C.

Despite the different solvents used to collect the NMR data for $[Rh_2(DTolF)_2\{d(GpG)\}]$ and free d(GpG), ($[Rh_2(DTolF)_2\{d(GpG)\}]$ is not soluble in D_2O only), the resonance of 5′-G H8 for the adduct is considerably downfield-shifted ($\Delta\delta$ ~1 ppm) as compared to free d(GpG). As will be inferred from the 2D NMR spectroscopic data (vide infra), the guanine bases in $[Rh_2(DTolF)_2\{d(GpG)\}]$ have a HH orientation (Scheme 4), and it has been established from platinum–d(GpG) adducts that HH dinucleotide adducts give rise to one or both H8 signals that are ~1 ppm

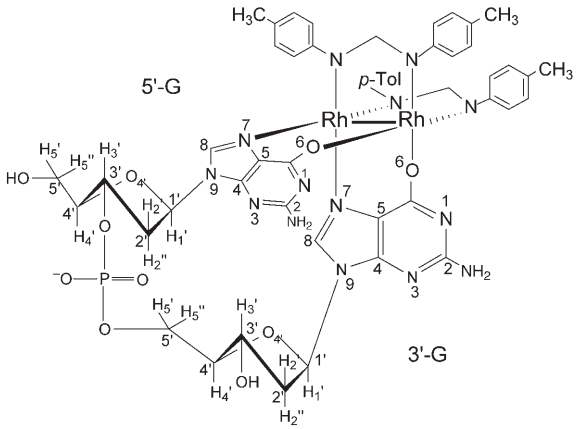

Scheme 4. Structure and numbering for $[Rh_2(DTolF)_2\{d(GpG)\}]$. Bond lengths are not scaled and angles between atoms are distorted to show the structure clearly.

downfield from free d(GpG).[29,33] The pH-dependence ^{1}H NMR titration for $[Rh_2(DTolF)_2\{d(GpG)\}]$, performed in CD_3CN (see Figure S1 in the Supporting Information), indicates the absence of protonation of the *N7* sites at low pH values, which corroborates binding of the metal to the *N7* sites. Moreover, in the pH-dependence ^{1}H NMR titration curves, inflection point(s) are observed at pK_a ~7.5 (see Figure S1 in the Supporting Information), which correspond to the (de)protonation(s) of the *N1* sites of the two bases. By applying the same argumentation for the pK_a values of the dinucleotide as for the 9-EtGuaH adduct (vide supra), it is inferred that the pK_a values of the *N1*-H sites in $[Rh_2(DTolF)_2\{d(GpG)\}]$ have decreased considerably compared to free d(GpG) (pK_a ~10.0 in D_2O;[22] the pK_a should be higher in CD_3CN[34]). The notable increase in the acidity of *N1-H* is attributed to the bidentate *N7/O6* binding of the guanine bases to the dirhodium unit.

In the aromatic region, there also is a triplet at $\delta =$ 7.47 ppm (with twice the intensity of each H8 resonance), which is ascribed to the two N-C*H*-N proton nuclei of the bridging formamidinate groups (Figure 2; the triplet is attributed to ^{1}H coupling to the two equivalent rhodium nuclei, $^3J\{^{103}Rh,^1H\} = 3.8$ Hz).

^{13}C NMR spectroscopy

For the aforementioned compounds, guanine binding to the dirhodium core through N7/*O6* was corroborated by means of ^{13}C NMR spectroscopy. In Table 2, a compendium of the

Table 1. ^{1}H and ^{31}P NMR chemical shifts (δ, ppm) for $[Rh_2(DTolF)_2\{d(GpG)\}]$.

d(GpG) species	G	H8	H1′	^3J(H1′,H2′)/ ^3J(H1′,H2″)[c]	H2′	H2″	H3′	H4′	H5′/H5″	Base sugar	^{31}P NMR[f]
$[Rh_2(DTolF)_2\{d(GpG)\}]$[a]	5′	8.64	6.12	0/6(d)	2.57	2.18	4.68	3.95	3.81/3.85[e]	*anti*	−2.38
	3′	7.82	6.19	0/14(d)	2.40[d]	2.40[d]	4.45	4.00	3.76/3.90[e]	*anti*	
d(GpG)[b]	5′	7.71	5.96		2.36	2.16	4.74	4.17	3.68[d]	*anti*	−4.00
	3′	8.00	6.08		2.77	2.47	4.77	4.18	4.09[d]	*anti*	

[a] 2D NMR spectra collected in CD_3CN/D_2O: 80/20% at 10°C. [b] 2D NMR spectra collected in D_2O at 5°C.[22] [c] In Hertz. [d] Overlapped resonances. [e] Not stereospecifically assigned. [f] Referenced to TMP at 0 ppm.

Table 2. ^{13}C NMR data (ppm) for 9-EtGuaH, d(GpG) and their dirhodium bis-formamidinate adducts.

Compound	Purine carbon atoms					DTolF carbon atoms			
	C6	C2	C4	C8	C5	N-*C*H-N	4°	1°	-CH_3
9-EtGuaH[a]	159.26	153.95	151.57	140.11	116.42				
$[Rh_2(DTolF)_2(CH_3CN)_6](BF_4)_2$[b]						169.88	135.19	129.68	20.84
							148.62	127.29	
$[Rh_2(DTolF)_2(9\text{-}EtGuaH)_2](BF_4)_2$[b,c,d]	163.00	154.09	149.74	144.78	[f]	169.73	148.73	130.03	20.91
	162.86	153.85	149.30	144.57		169.05	148.40	129.94	20.80
							135.37	127.27	
							135.07	127.07	
d(GpG)[a]	158.99	153.84	151.29	137.91	116.78				
	158.36	153.77	150.93	137.21	115.71				
$[Rh_2(DTolF)_2\{d(GpG)\}]$[e]	163.01	154.64	152.57	137.52	[f]	169.72	148.55	129.96	20.81
	162.66	154.23	152.28	137.48		169.57	148.45	129.71	20.78
							135.36	127.25	
							134.84	127.01	

[a] ^{13}C NMR spectra collected in D_2O.[22] [b] ^{13}C NMR data collected in CD_3CN. [c] Both isomers. [d] The ^{13}C NMR resonances for the CH_3 and -CH_2- groups of 9-EtGuaH appear at $\delta = 15.17$ and 40.79 ppm, respectively (for both isomers). [e] ^{13}C NMR data collected in CD_3CN/D_2O 80/20 %. [f] The resonances could not be assigned accurately due to the broad peak at $\delta = 118.2$ ppm from the residual carbon impurity in CD_3CN.

^{13}C NMR chemical shift values for 9-EtGuaH, d(GpG) and their bis-formamidinate dirhodium adducts is reported.

For the dirhodium compounds, the ^{13}C NMR resonances were assigned in conjunction with the ^{13}C{APT}[57,58] technique. In the ^{13}C{APT} spectra, the resonances attributed to carbon atoms with an odd number of attached protons (e.g., CH and CH_3 groups) face downwards, whereas the resonances due to carbon atoms with an even number of attached protons (including quaternary carbon atoms) face upwards. To this effect, for the $[Rh_2(DTolF)_2(NCCH_3)_6](BF_4)_2$ complex, the ^{13}C NMR resonances (Table 2) attributed to the formamidinate group N-*C*H-N ($\delta = 169.88$ ppm; this group gives rise to the most downfield ^{13}C NMR resonance in the spectrum) as well as the *ortho*- and *meta*-carbon atoms (1°) of the tolyl rings ($\delta = 127.29$, 129.68 ppm) face downwards.[36,37] On the other hand, the quaternary carbon atoms (4°) of the tolyl rings ($\delta = 135.19$, 148.62 ppm) face upwards.[36]

Although the ^{13}C NMR data for 9-EtGuaH and free d(GpG) were collected in a different solvent from their dirhodium bis-formamidinate complexes, a comparison of the chemical shifts between the free ligands and the complexes is still viable. For both $[Rh_2(DTolF)_2(9\text{-}EtGuaH)_2](BF_4)_2$ and $[Rh_2(DTolF)_2\{d(GpG)\}]$, the ^{13}C NMR resonances of the C6 nuclei have shifted downfield by $\Delta\delta \sim 4.0$ ppm compared to the corresponding resonances of the unbound ligands (Table 2). Since the ^{13}C NMR spectra of both $[Rh_2(DTolF)_2(9\text{-}EtGuaH)_2](BF_4)_2$ and $[Rh_2(DTolF)_2\{d(GpG)\}]$ were acquired at pH values below the inflection points for *N1* (de)protonation (pK_a values 7.3 and 7.5, respectively; vide supra), the *N1* positions of the bases are protonated and thus the downfield shifts of the C6 ^{13}C NMR resonances, due to *O6* binding of the bases to the rhodium centers, are not as pronounced as they would have been if the *N1* sites were deprotonated. The $\Delta\delta \sim 4.0$ ppm downfield shifts observed for the ^{13}C NMR resonances of the C6 nuclei for $[Rh_2(DTolF)_2(9\text{-}EtGuaH)_2](BF_4)_2$ and $[Rh_2(DTolF)_2\{d(GpG)\}]$ are comparable to the downfield shifts of the corresponding resonances for $[Rh_2(O_2CCH_3)_2(9\text{-}EtGuaH)_2]$,[22] $[Rh_2(O_2CCH_3)_2(5'\text{-}GMP)_2]$[25] and $[Rh_2(O_2CCH_3)_2\{d(pGpG)\}]$[25] at pH 4, wherein the *N1* sites of the guanine bases are protonated and the bases are binding to the dirhodium units through *N7/O6*. In the bis-formamidinate complexes, the ^{13}C NMR resonances for C2 have not been essentially affected, because C2 is sensitive to deprotonation only, whereas C6 is sensitive to *O6* complexation as well as *N1* deprotonation.[38–40] The C5 nuclei for the dirhodium compounds being studied experienced only small *downfield* shifts upon complexation as reported in the literature for metal *O6* binding;[39] the downfield impact on C5 upon *O6* binding may be partially counterbalanced by the expected upfield shift of about 3 ppm (observed in cisplatin adducts) due to *N7* binding of the metal.[39–42] The ^{13}C NMR resonance of the C8 carbon usually experiences a downfield shift of about 3 ppm upon *N7* metal coordination.[41–43] Although this trend is followed by the 9-EtGuaH adducts with dirhodium bis-formamidinate ($\Delta\delta \sim 4$ ppm; Table 2), for the tethered d(GpG) adduct, the expected downfield shift of C8 was not observed as in a few other reported cases.[22,25,44,45] In the case of the single-stranded [d(TG*G*T)-*N7*/*N7*]-Pt(en) complex, it is attributed to the "nonideal" overlap of the N7 lone pairs of both guanine bases with the metal center due to metal-induced distortion of the DNA structure, as well as to heavy-atom anisotropic effects of platinum on the ^{13}C NMR chemical shifts.[44]

2D ^{1}H NMR spectroscopy

2D ROESY, DQF-COSY and [^{1}H–^{31}P] HETCOR NMR spectra were collected to assess the structural features and assign the nonexchangeable proton resonances of the dirhodium bis-formamidinate d(GpG) species (Table 1).

In the aromatic region of the 2D ROESY NMR spectrum of $[Rh_2(DTolF)_2\{d(GpG)\}]$, the two H8 resonances are well

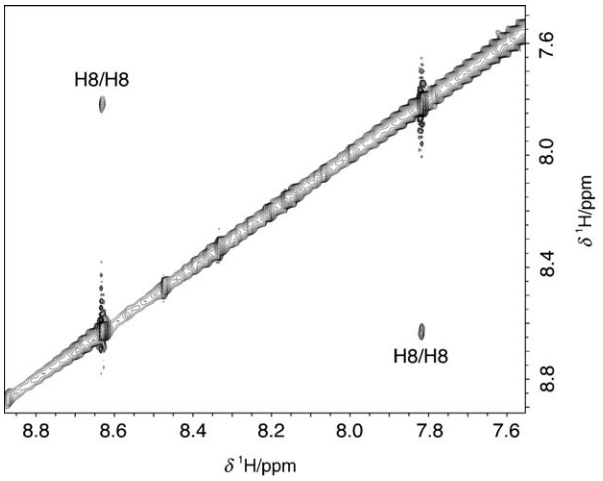

Figure 3. H8/H8 region of the 2D ROESY NMR spectrum for $[Rh_2(DTolF)_2\{d(GpG)\}]$ in CD_3CN/D_2O 80:20% at 10°C.

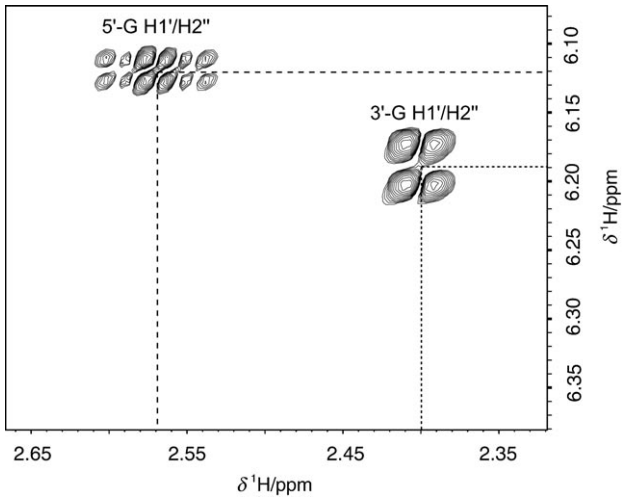

Figure 4. H1′ and H2′/H2″ region of the 2D $[^1H–^1H]$ DQF-COSY NMR spectrum for $[Rh_2(DTolF)_2\{d(GpG)\}]$ in CD_3CN/D_2O 80:20% at 10°C. The 5′-G and 3′-G cross-peaks are indicated with a medium dash (-----) and a dotted line (····), respectively.

separated and exhibit intense H8/H8 ROE cross-peaks (Figure 3). These observations strongly support HH base orientation, which has been observed for the bis-acetate dirhodium[22,25] and platinum compounds.[28–31,33] Head-to-tail (HT) conformers lack these cross-peaks due to long H8/H8 distances.[28–31,33]

The set of H8 ^1H NMR resonances for $[Rh_2(DTolF)_2\{d(GpG)\}]$ are assigned to the 5′-G and 3′-G residues by the following assessment: the downfield H8 resonance ($\delta =$ 8.64 ppm) exhibits a H8/H3′ cross-peak in the 2D ROESY spectrum and this H3′ ($\delta = 4.68$ ppm) has a cross-peak to the phosphodiester ^{31}P NMR resonance ($\delta = -2.38$ ppm) in the $[^1H–^{31}P]$ HETCOR spectrum, leading to an unequivocal assignment of the downfield H8 resonance at $\delta = 8.64$ ppm to 5′-G, whereas H5′/H5″-^{31}P and H4′-^{31}P cross-peaks are observed for the 3′-G only.[22,25,28–31] The 3′-G residue exhibits strong H8/H2′/H2″ ROE cross-peaks and both sugar residues exhibit weak H8/H1′ ROE cross-peaks, which are features consistent with *anti* glycosidic torsion angles.[22,25,28–31,33] The 5′-G exhibits a strong H8/H2″ ROE cross-peak; the expected H8/H2′ ROE cross-peak, however, is absent. A possible explanation is that the sugar conformation is "*high-anti*", a variation of the *anti*-conformation resulting from a near eclipse of the C1′–C2′ sugar bond with the N9–C8 bond of the purine.[46] Furthermore, the 5′-G exhibits a strong H8/H3′ ROE cross-peak along with H1′–H2″ (no H1′–H2′) DQF-COSY cross-peaks and a doublet coupling pattern for its H1′ in the $[^1H–^1H]$ DQF-COSY spectrum (Figure 4); these findings imply a C3′-*endo* (N-type) sugar conformation for 5′-G.[22,25,28–31,33,46,47] Residue 3′-G also exhibits a strong H8/H3′ ROE cross-peak (although weaker than that for 5′-G), a H1′-H2″ DQF-COSY cross-peak (the resonances for H2′ and H2″ coincide at $\delta = 2.40$ ppm; Table 1) and a doublet coupling pattern for its H1′ in the $[^1H–^1H]$ DQF-COSY spectrum (Figure 4), which indicate a C3′-*endo* (N-type) sugar conformation for the 3′-G residue as well.[22,25,28–31,33,46,47] It is unprecedented for a dirhodium d(GpG) HH cross-linked adduct to have both deoxyribose residues in the C3′-*endo* (N-type) conformation.[22,25]

^{31}P NMR spectroscopy

$[Rh_2(DTolF)_2\{d(GpG)\}]$: The 1D ^{31}P NMR spectrum displays a resonance at $\delta = -2.38$ ppm (Table 1), which is located downfield from that of the unbound dinucleotide d(GpG) ($\delta = -4.00$ ppm). Typically, for HH isomers, the phosphate groups resonate about 1 ppm downfield from the unbound dinucleotide.[22,25,33] Downfield shifts of the ^{31}P NMR resonances in DNA usually indicate an increase in the unwinding angle characterized by changes in the R-O-P-OR′ torsion angles.[48] The downfield ^{31}P NMR chemical shifts, observed for d(GpG) containing oligonucleotide adducts with platinum and other metals imply that, when adjacent guanine residues bind to the metal, an extension of the conformation about the diester bond between the G bases occurs.[49]

Molecular modeling

Models of the dirhodium bis-formamidinate adducts were constructed and subjected to simulated annealing calculations. The conformational features of the adducts determined by NMR spectroscopy were reproduced well by the calculations. The differences in energy values have been interpreted in conjunction with the NMR spectroscopic data. The HH and HT models constructed for $[Rh_2(DTolF)_2(9\text{-}EtGuaH)_2]^{2+}$ are nearly isoenergetic (199.6 and 199.2 kcal mol^{-1}, respectively), a result that supports their presence in 1:1 ratio in solution (as inferred from the ^1H NMR spectroscopic data).

Initial HH1R, HH1L, HH2L conformers for the tethered adduct $[Rh_2(DTolF)_2\{d(GpG)\}]$ were independently con-

Table 3. Summary of lowest energy dirhodium adducts with d(GpG) and d(pGpG).

Model	Percent [%][a]	Energy [kcal mol^{-1}]	χ [°][b]		P [°][c]		Dominant 3′-G sugar type	5′-G H8/ 3′-G H8 [Å]	3′-G/5′-G Dihedral angle [°][d]
			5′-G	3′-G	5′-G	3′-G			
$[Rh_2(DTolF)_2\{d(GpG)\}]$ HH1R[a]	100	300.7	−137	−146	20	12	N	3.30	75.9
$[Rh_2(DTolF)_2\{d(GpG)\}]$ HH2L	0	303.1	−1.2	−166	5	14	N	3.51	73.7
$[Rh_2(O_2CCH_3)_2\{d(GpG)\}]$ HH1R[a,e]	74	255.6	−129	−125	28	126	S	2.97	75.0
$[Rh_2(O_2CCH_3)_2\{d(GpG)\}]$ HH2R[a,e]	24	256.7	18[f]	67[f]	19	40[g]	S	2.96	66.0
$[Rh_2(O_2CCH_3)_2\{d(pGpG)\}]$ HH1L[a,h]	100	329.5	−134	−45[f]	27	144	S	3.12	81.3

[a] Experimentally observed. [b] χ = O4′-C1′-N9-C4; $|\chi| > 90°$ and $|\chi| < 90°$ correspond to the *anti* and *syn* range respectively, for torsion angles $-180° < \chi < +180°$. [c] P = pseudorotation phase angle calculated from the equation $\tan P = ((\nu_4 + \nu_1) - (\nu_3 + \nu_0)/(2\nu_2(\sin 36° + \sin 72°))$ ($\nu_{0\text{-}4}$ are endocyclic sugar torsion angles; $0° \le P \le 36°$ ($\pm 18°$) corresponds to an N sugar, while $144° \le P \le 190°$ (± 18 °) indicates an S sugar; if $\nu_2 < 0$, $P = P + 180$. [d] Dihedral angles between 5′-G and 3′-G were calculated by using atoms N1, N3, N7 of each purine ring. [e] Reference [22]. [f] These angles are in the range to be considered *syn*; however, the H8–H2′ distance is less than the H8–H1′ distance and other low-energy structures have χ angles in the *anti* range. [g] In most other low energy structures of these variants, the 3′-G sugar rings have an S-type conformation. [h] Reference [25].

structed and subjected to simulated annealing calculations, because starting right- and left-handed models produced minimized conformers with the same canting as the original models only. The lowest energy HH1R variant (Figure 5) is 2.4 kcal mol^{-1} more stable than the lowest energy HH2L variant (Table 3). The lowest energy HH1R variant (Figure 5) is lower than the lowest energy HH1L conformer by 2.0 kcal mol^{-1} (the HH1L conformers were not further considered because their presence is not supported by the NMR data). For the HH1R conformers, the H8/H8 distances are in the range ~3.2–3.4 Å (Table 3), thus corroborating relatively intense H8/H8 cross-peaks in the 2D ROESY NMR spectrum (Figure 3; vide supra). Both the 5′-G and 3′-G sugar residues are in the *anti*-orientation with respect to the glycosyl bonds, in accordance with the NMR data (vide supra). The measured interproton H8/H3′ distances (2.34 and 3.09 Å for 5′-G and 3′-G, respectively), for the lowest energy HH1R conformer, are in accord with the strong H8/H3′ ROE NMR cross-peaks and thus N-type conformations for both the 5′-G and 3′-G deoxyribose rings. Since an N-type conformation for the 3′-G deoxyribose is rarely encountered in platinum complexes,[29,46] the conformations of the 3′-G residues for 500 minimized HH1R $[Rh_2(DTolF)_2\{d(GpG)\}]$ models were considered. It was found that 57% of the 3′-G sugars are in an N-type conformation. If the HH1R $[Rh_2(NHCHNH)_2\{d(GpG)\}]$ model is constructed (by replacing the tolyl groups with hydrogen atoms) and minimized, 53% of the 3′-G sugars are in an N-type conformation.

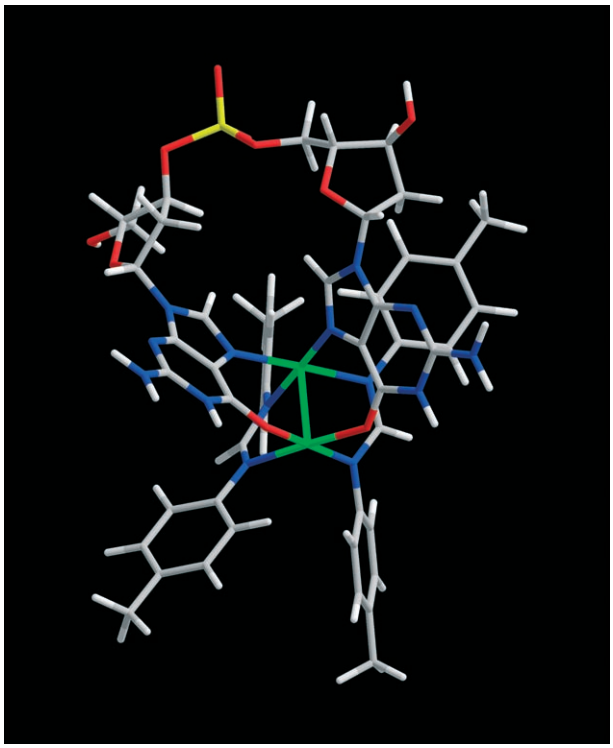

Figure 5. Lowest energy conformer for the experimentally observed HH1R variant of $[Rh_2(DTolF)_2\{d(GpG)\}]$, resulting from simulated annealing calculations. The 5′-G residue is positioned to the left and 3′-G is the more canted base. Color code: Rh green, N blue, O red, P yellow, C gray, H white.

Discussion

As in the case of $[Rh_2(O_2CCH_3)_4]$,[19,20,22] reaction of $[Rh_2(DTolF)_2(CH_3CN)_6](BF_4)_2$ with 9-EtGuaH proceeds by formation of HH to HT isomers in 1:1 ratio, wherein 9-EtGuaH adopts equatorial bridging interactions through the *N7/O6* atoms spanning the dirhodium unit in a *cis* disposition.[23] The presence of the two isomers in equal amounts (a finding reproduced by the simulated annealing calculations) is based on the ^{1}H NMR spectroscopic data. The pH-dependence study of the H8 ^{1}H NMR resonance for $[Rh_2(DTolF)_2(9\text{-EtGuaH})_2](BF_4)_2$ in CD_3CN (Figure 1), indicates the absence of *N7* protonation at low pH (due to *N7* binding to the metal) and a substantial enhancement in the acidity of *N1-H*, (the pK_a value has decreased to ~7.3 as compared to ~9.5 for unbound 9-EtGuaH and ~8.5 for *N7 only* bound adducts), due to the *O6* binding of the base to the dirhodium unit.[22,25] The pH-dependence ^{1}H NMR titration curves for the H8 resonances of $[Rh_2(DTolF)_2\{d(GpG)\}]$ (see

Figure S1 in the Supporting Information) closely resemble those of $[Rh_2(DTolF)_2(9\text{-}EtGuaH)_2](BF_4)_2$ (Figure 1), that is, no *N7* protonation is observed at low pH and the pK_a values of *N1-H* deprotonation have decreased to ~7.5 for both 5′-G H8 and 3′-G H8. The latter effects are induced by purine binding to the rhodium centers through *N7/O6*.[22,25] For both the $[Rh_2(DTolF)_2(9\text{-}EtGuaH)_2](BF_4)_2$ and $[Rh_2(DTolF)_2\{d(GpG)\}]$ adducts, the downfield shifts by $\Delta\delta \sim 4.0$ ppm of the ^{13}C NMR resonances for the C6 nuclei as compared to the corresponding resonances of the unbound ligands, further corroborate *N7/O6* binding.[22,25]

In $[Rh_2(DTolF)_2\{d(GpG)\}]$, the two dinucleotide H8 protons are nonequivalent. In addition to the deshielding effect of the metal on both rings, the more canted base experiences an upfield shifting effect due to the ring-current anisotropy of the other *cis* base. The guanine bases are not oriented exactly perpendicular to the coordination plane, and the degree and direction of canting depends on the carrier ligands, the presence of a linkage between the bases, the sugar type (deoxyribose or ribose), the presence of a 5′-flanking residue, and the single- or double-stranded character of the DNA.[33,50] The $[Rh_2(DTolF)_2\{d(GpG)\}]$ adduct gives rise to well-dispersed H8 proton resonances and intense H8/H8 ROE cross-peaks, which are consistent with HH conformers.[22,25,28–31,33] The 2D NMR spectroscopic data support the assignment of the upfield and downfield H8 resonances to the 3′-G and 5′-G H8 protons, respectively (Table 1; vide supra). Based on the recently assessed rules for base canting,[28,29] in $[Rh_2(DTolF)_2\{d(GpG)\}]$, 3′-G is more canted than 5′-G (Scheme 3; the H8 resonance of the more canted base moves upfield due to the ring current effect of the less canted base; Figure 2). Taking into consideration both the experimental evidence from the NMR spectroscopic data as well as the molecular modeling results (Table 3), the *only* $[Rh_2(DTolF)_2\{d(GpG)\}]$ conformer present in solution is assigned to the right-handed variant HH1R (Scheme 3), which has precedent for dirhodium dinucleotide adducts; when acetate groups support the Rh–Rh bond, two conformers HH1R (75%) and HH2R (25%) $[Rh_2(O_2CCH_3)_2\{d(GpG)\}]$ are formed.[22] In the case of the $[Rh_2(DTolF)_2\{d(GpG)\}]$ adduct, however, the bulk and the nonlabile character of the formamidinate compared to the acetate bridging groups,[51] slow down the possible dynamic processes for the adduct[28] and thus eliminate the formation of the minor variant HH2R observed for the acetate.[22] The $[Rh_2(DTolF)_2\{d(GpG)\}]$ HH1R conformer is unusual in the sense that it is an R minihelix variant (with opposite chemical shift relationship of the 3′-G and 5′-G H8 protons as compared to *cis*-$[Pt(NH_3)_2\{d(GpG)\}]$). HH1L variants of single-stranded d(GpG) platinum adducts appear to be dominant in solution,[26,27] except for a few other reported cases.[28,30,32] In duplexes with the *cis*-$[Pt(NH_3)_2\{d(GpG)\}]$ moiety, however, the HH1R variants appear to dominate.[26,27] In this respect, the d(GpG) dirhodium HH1R variants are better models than *cis*-$[Pt(NH_3)_2\{d(GpG)\}]$ for the duplex DNA cross-link lesion.[28–31,50] The H8 chemical shifts for HH1R $[Rh_2(DTolF)_2\{d(GpG)\}]$ are upfield shifted by about 0.6 ppm as compared to the corresponding H8 chemical shifts of HH1R $[Rh_2(O_2CCH_3)_2\{d(GpG)\}]$;[22] thus, the rhodium(II) centers in $[Rh_2(O_2CCH_3)_2\{d(GpG)\}]$ exert a greater inductive effect,[33] which is attributed to the poorer electron-donating ability of the acetate as compared to the formamidinate bridging groups.[1]

The 2D NMR spectroscopic data of the $[Rh_2(DTolF)_2\{d(GpG)\}]$ adduct support *anti*-orientation of both sugar residues about the glycosyl bonds and a repuckering of the 5′-G deoxyribose residue to N (C3′-*endo*). These features bear close resemblance to those of *cis*-$[Pt(NH_3)_2\{d(GpG)\}]$, which is a HH cross-linked adduct with *anti/anti* 5′-G and 3′-G sugar residues in the N and S conformations, respectively. The N-pucker for the 5′-G is universal in such cross-links.[33] For the $[Rh_2(DTolF)_2\{d(GpG)\}]$ adduct, however, the 3′-G sugar is also in the N (C3′-*endo*) conformation. In the case of platinum adducts, N-type conformations for both deoxyribose residues have only been reported for HT *(S,R,R,S)*-$[BipPt\{d(GpG)\}]$[29] and *trans*-$[PtCl(NH_3)_2\}_2\{\mu\text{-}NH_2(CH_2)_6NH_2\}\{d(GpG)\}]$.[46] It is unprecedented for a dirhodium d(GpG) HH cross-linked adduct to have both deoxyribose residues in the C3′-*endo* (N-type) conformation (Table 3).[22,25] It is known that several steric and electronic factors[52] affect the preferred furanose puckering modes, such as the C3′ furanose substituent, as well as the modifications of the base.[53,54] In the case of $[Rh_2(DTolF)_2\{d(GpG)\}]$, most likely electronic changes to the base and steric factors, due to the formamidinate bridging groups, are responsible for the dominance of an N-type 3′-G deoxyribose ring.

Conclusion

The present study supports equatorial *N7/O6* binding of GG containing DNA fragments spanning the Rh–Rh bond in the $[Rh_2(DTolF)_2\{d(GpG)\}]$ adduct. The guanine bases are almost completely destacked upon coordination to the metal centers (3′-G/5′-G dihedral angle 75.9°) and favorably poised to accommodate the bidentate *N7/O6* binding to the dirhodium core. The tethering of the guanine bases dictates the HH nature of the $[Rh_2(DTolF)_2\{d(GpG)\}]$ adduct, whereas the formamidinate bridging groups favor *one right-handed* HH1R conformer in solution, as opposed to two conformers HH1R (75%) and HH2R (25%) in the case of $[Rh_2(O_2CCH_3)_2\{d(GpG)\}]$.[22] In $[Rh_2(DTolF)_2\{d(GpG)\}]$, the presence of the bulky, nonlabile and electron-donating formamidinate bridging groups induces electronic and conformational changes to the dirhodium d(GpG) adduct that are different, in some aspects, from those of the acetate. Clearly, tailoring the bridging groups on the dirhodium core affects the nature of the preferred DNA adducts. A notable point of this study relates to the *N7/O6* binding to the dirhodium core with the consequential large decrease of the pK_a value for *N1-H* deprotonation. This *N7/O6* binding mode influences the Watson–Crick hydrogen bonding of the bases and shifts the pK_a value into the physiological pH range.[55,56] In light of the biological activity of *cis*-$[Rh_2$-

$(DTolF)_2(O_2CCF_3)_2(H_2O)_2]$, the implications of its interactions with DNA fragments remain to be determined.

Experimental Section

Materials: The reagent 9-ethylguanine (9-EtGuaH) was purchased from Sigma. The starting material $RhCl_3 \cdot x H_2O$ was obtained from Pressure Chemical Co. (Pittsburgh, PA) and was used without further purification. The compound *cis*-$[Rh_2(DTolF)_2(NCCH_3)_6](BF_4)_2$ was prepared according to literature procedures.[23] The dinucleotide d(GpG), which was purchased as the crude 5′-O-dimethoxytrityl(DMT)-protected material from the Gene Technologies Laboratory at Texas A&M University, was purified by reverse-phase HPLC and was used as the sodium salt. Concentrations of the dinucleotide were determined by UV spectroscopy (Shimadzu UV 1601PC spectrophotometer) at 252 nm ($\varepsilon_{252} = 2.5 \times 10^4\,M^{-1}\,cm^{-1}$). Deuterium oxide ($D_2O$, 99.996%), deuterated acetonitrile (CD_3CN, 99.8%), deuterium chloride (DCl, 99.5%), and sodium deuteroxide (NaOD, 99.5%) were purchased from Cambridge Isotope Laboratories. TMP {$(CH_3O)_3PO$} was purchased from Aldrich.

Syntheses

***cis*-$[Rh_2(DTolF)_2(9\text{-}EtGuaH)_2](BF_4)_2$**.[23] In a typical reaction, a slurry of 9-EtGuaH (75 mg, 0.42 mmol) in acetone (3 mL) was added to a brown solution of $[Rh_2(DTolF)_2(NCCH_3)_6](BF_4)_2$ (225 mg, 0.21 mmol) in CH_3CN (15 mL) and the mixture was heated under reflux for a few hours (during this time the solution turned to green). The reaction solution was filtered and the filtrate was evaporated in vacuo to produce a green solid. ^1H NMR (500 MHz, CD_3CN, 20 °C) $\delta = 8.08$ (s, 2H; H8), 8.05 (s, 2H; H8), 7.55 (t, $^3J(^{103}Rh,^1H) = 3.8$ Hz, 2H; N-C*H*-N), 7.41 (t, $^3J(^{103}Rh,^1H) = 3.8$ Hz, 2H; N-C*H*-N), 6.99 (m, tolyl), 4.07 (q, overlapping, CH_2), 2.24 (s, 12H; CH_3(tolyl)), 2.21 (s, 12H; CH_3(tolyl)), 1.95 (s, *ax*-CH_3CN), 1.39 (t, 6H; CH_3), 1.31 ppm (t, 6H; CH_3); MS-ESI: *m/z* (%): 1009.4 (100) $[Rh_2(DTolF)_2(9\text{-}EtGuaH)_2\text{-}1]^+$.

$[Rh_2(DTolF)_2\{d(GpG)\}]$: In a typical reaction, $[Rh_2(DTolF)_2(NCCH_3)_6](BF_4)_2$ (2.3 μmol) in CD_3CN (200 μL, brown solution) was treated with d(GpG) (2.3 μmol) in D_2O (50 μL). Upon mixing the two solutions, a white precipitate formed. After incubating the sample at 37 °C for a few days, the white solid dissolved completely and the color of the solution changed from brown to green. The progress of the reaction was monitored by ^1H NMR spectroscopy until no free d(GpG) could be detected. The reaction was complete in about eight days. MS-ESI: *m/z*: 1246.9 (see Figure S2 in the Supporting Information).

Instrumentation: The 1D ^1H NMR spectra were recorded on a 500-MHz Varian Inova spectrometer with a 5-mm switchable probehead. The ^1H NMR spectra were typically recorded with a 5000 Hz sweep width and 32 K data points. A presaturation pulse to suppress the water peak was used when necessary. The 1D $^{13}C\{^1H\}$ and the attached proton test[57,58] ($^{13}C\{APT\}$) NMR spectra were recorded on a 500-MHz Varian Inova spectrometer operating at 125.76 MHz for ^{13}C. The 1D ^{31}P NMR spectra were recorded on a Varian 300-MHz spectrometer operating at 121.43 MHz for ^{31}P. The ^1H NMR spectra were referenced to the residual proton impurity of CD_3CN, whereas the ^{13}C NMR spectra were referenced to the residual carbon impurities of CD_3CN. Trimethyl phosphate (TMP) (0 ppm) was used as an external reference for the ^{31}P NMR spectra. The 1D NMR data were processed using the Varian VNMR 6.1b software.

The 2D NMR data were collected at 10 °C on a Varian Inova 500-MHz spectrometer equipped with a triple-axis gradient penta probe. In general, the homonuclear experiments were performed with a spectral width of about 5000 Hz in both dimensions, whereas some high-resolution 2D $[^1H\text{–}^1H]$ DQF-COSY spectra were collected with a 3000 Hz spectral width. 2D $[^1H\text{–}^1H]$ ROESY (rotating-frame Overhauser enhancement spectroscopy) spectra were collected with a mixing time of 300 ms. A minimum of 2048 points was collected in t_2 with at least 256 points in t_1 and 64 scans per increment. 2D $[^1H\text{–}^1H]$ DQF-COSY (double-quantum filtered correlation spectroscopy) spectra, collected with ^{31}P decoupling in both dimensions, resulted in a 1260×600 data matrix with 32 scans per increment. 2D $[^1H\text{–}^{31}P]$ HETCOR (heteronuclear shift correlation) experiments were collected with 2048 points in t_2, 128 points in t_1 with 112 scans per increment. The ^{31}P NMR spectral width was approximately 2000 Hz. All data sets were processed by using a 90° phase-shifted sine-bell apodization function and were zero-filled. The baselines were corrected with first or second order polynomials. Two-dimensional (2D) NMR data were processed by using the program nmrPipe.[59]

The pH values of the samples were recorded on a Corning pH meter 430 equipped with a MI412 microelectrode probe by Microelectrodes, Inc. The pH dependence of the chemical shifts of the purine H8 nuclei was monitored by adding trace amounts of DCl and NaOD solutions. No correction was applied to the pH values for deuterium isotope effects on the glass electrode. The pH titration curves were fitted to the Henderson–Hasselbalch equation using the program KALEIDAGRAPH, with the assumption that the observed chemical shifts are weighted averages according to the populations of the protonated and deprotonated species.

MALDI (matrix-assisted laser desorption ionization) mass spectra were acquired by using an Applied Biosystems Voyager Elite XL mass spectrometer.

Molecular modeling: Molecular modeling results were obtained by using the software package Cerius^2 4.6 (Accelrys Inc., San Diego). To sample the conformational space of each compound, simulated annealing calculations in the gas phase were performed by using the open force field (OFF) program, with a modified version of the universal force field (UFF).[60–62] The simulated annealing was carried out for 80.0 ps, over a temperature range of 300–500 K, with $\Delta T = 50$ K, using the Nosé temperature thermostat, a relaxation time of 0.05 ps and a time step of 0.001 ps. The compounds were minimized (quenched) after each annealing cycle, producing 500 minimized structures. UFF is parameterized for octahedral rhodium(III), whereas the molecules in the present study are metal–metal-bonded rhodium(II) compounds with a paddlewheel structure. In order to account for the difference in the oxidation state and the coordination environment of the metal for this type of complexes, the appropriate valence bond parameter was previously developed.[22,25]

Acknowledgements

Dr. K. M. Koshlap is acknowledged for assistance with the 2D NMR data collection and Dr. S. K. Silber for advice on the APT ^{13}C NMR data. We thank Dr. Lisa Pérez for assistance with the molecular modeling; the Laboratory for Molecular Simulations at Texas A&M University is acknowledged for providing software and computer time. Use of the TAMU/LBMS-Applications Laboratory (Laboratory of Biological Mass Spectroscopy) is also acknowledged. The NMR instrumentation in the Chemistry Department at Texas A&M University was funded by NSF (CHE-0077917). The NMR instrumentation in the Biomolecular NMR Laboratory at Texas A&M University was supported by a grant from the National Science Foundation (DBI-9970232) and the Texas A&M University System. KRD thanks the Welch Foundation (A-1449) for financial support.

[1] H. T. Chifotides, K. R. Dunbar, "Rhodium Compounds", in *Multiple Bonds Between Metal Atoms*, *Chapter 12* (Eds.: F. A. Cotton, C. Murillo, R. A. Walton), Springer, New York, **2005**, pp. 465–589.
[2] R. G. Hughes, J. L. Bear, A. P. Kimball, *Proc. Am. Assoc. Cancer Res.* **1972**, *13*, 120.
[3] R. A. Howard, A. P. Kimball, J. L. Bear, *Cancer Res.* **1979**, *39*, 2568–2573.
[4] A. Erck, L. Rainen, J. Whileyman, I.-M. Chang, A. P. Kimball, J. L. Bear, *Proc. Soc. Exp. Biol. Med.* **1974**, *145*, 1278–1283.
[5] J. L. Bear, H. B. Gray, Jr., L. Rainen, I. M. Chang, R. Howard, G. Serio, A. P. Kimball, *Cancer Chemother. Rep.* **1975**, *59*, 611–620.
[6] R. A. Howard, E. Sherwood, A. Erck, A. P. Kimball, J. L. Bear, *J. Med. Chem.* **1977**, *20*, 943–946.

[7] S. Zyngier, E. Kimura, R. Najjar, *Braz. J. Med. Biol. Res.* **1989**, *22*, 337–344.
[8] J. L. Bear *Precious Metals 1985: Proceedings of the Ninth International Precious Metals Conference* (Eds.: E. D. Zysk, J. A. Bonucci), Int. Precious Metals, Allentown, PA, **1986**, 337–344.
[9] J. M. Asara, J. S. Hess, E. Lozada, K. R. Dunbar, J. Allison, *J. Am. Chem. Soc.* **2000**, *122*, 8–13.
[10] H. T. Chifotides, J. M. Koomen, M. Kang, K. R. Dunbar, S. Tichy, D. H. Russell, *Inorg. Chem.* **2004**, *43*, 6177–6187.
[11] S. U. Dunham, H. T. Chifotides, S. Mikulski, A. E. Burr, K. R. Dunbar, *Biochemistry* **2005**, *44*, 996–1003.
[12] H. T. Chifotides, K. R. Dunbar, *Acc. Chem. Res.* **2005**, *38*, 146–156.
[13] P. N. Rao, M. L. Smith, S. Pathak, R. A. Howard, J. L. Bear, *J. Natl. Cancer Inst.* **1980**, *64*, 905–911.
[14] L. D. Dale, T. M. Dyson, D. A. Tocher, J. H. Tocher, D. I. Edwards, *Anti-Cancer Drug Des.* **1989**, *4*, 295.
[15] K. Sorasaenee, P. K.-L. Fu, A. M. Angeles-Boza, K. R. Dunbar, C. Turro, *Inorg. Chem.* **2003**, *42*, 1267–1271.
[16] H. T. Chifotides, P. K.-L. Fu, K. R. Dunbar, C. Turro, *Inorg. Chem.* **2004**, *43*, 1175–1183.
[17] P. Piraino, G. Tresoldi, S. Lo Schiavo, *Inorg. Chim. Acta* **1993**, *203*, 101–105.
[18] V. Fimiani, T. Ainis, A. Cavallaro, P. Piraino, *J. Chemother.* **1990**, *2*, 319–326.
[19] K. R. Dunbar, J. H. Matonic, V. P. Saharan, C. A. Crawford, G. Christou, *J. Am. Chem. Soc.* **1994**, *116*, 2201–2202.
[20] C. A. Crawford, E. F. Day, V. P. Saharan, K. Folting, J. C. Huffman, K. R. Dunbar, G. Christou, *Chem. Commun.* **1996**, 1113–1114.
[21] For dirhodium adducts with bridging ligands possessing different types of donor atoms, that is, 9-EtGH, the compound is designated as HH or HT, according to whether the identical atoms of the two ligands are bound to the same or to opposite metal atoms, respectively.
[22] H. T. Chifotides, K. M. Koshlap, L. M. Pérez, K. R. Dunbar, *J. Am. Chem. Soc.* **2003**, *125*, 10703–10713.
[23] K. V. Catalan, J. S. Hess, M. M. Maloney, D. J. Mindiola, D. L. Ward, K. R. Dunbar, *Inorg. Chem.* **1999**, *38*, 3904–3913.
[24] H. T. Chifotides, K. V. Catalan, K. R. Dunbar, *Inorg. Chem.* **2003**, *42*, 8739–8747.
[25] H. T. Chifotides, K. M. Koshlap, L. M. Pérez, K. R. Dunbar, *J. Am. Chem. Soc.* **2003**, *125*, 10714–10724.
[26] J. Kozelka, M.-H. Fouchet, J.-C. Chottard, *Eur. J. Biochem.* **1992**, *205*, 895–906.
[27] D. Lemaire, M.-H. Fouchet, J. Kozelka, *J. Inorg. Biochem.* **1994**, *53*, 261–271.
[28] S. O. Ano, F. P. Intini, G. Natile, L. G. Marzilli, *J. Am. Chem. Soc.* **1998**, *120*, 12017–12022.
[29] L. G. Marzilli, S. O. Ano, F. P. Intini, G. Natile, *J. Am. Chem. Soc.* **1999**, *121*, 9133–9142, and references therein.
[30] K. M. Williams, L. Cerasino, G. Natile, L. G. Marzilli, *J. Am. Chem. Soc.* **2000**, *122*, 8021–8030.
[31] S. T. Sullivan, A. Ciccarese, F. P. Fanizzi, L. G. Marzilli, *J. Am. Chem. Soc.* **2001**, *123*, 9345–9355, and references therein.
[32] T. W. Hambley, E. C. H. Ling, B. A. Messerle, *Inorg. Chem.* **1996**, *35*, 4663–4668.
[33] D. Bhattacharyya, P. Marzilli, L. G. Marzilli, *Inorg. Chem.* **2005**, *44*, 7644–7651, and references therein.
[34] M. Rosés, *J. Chromatogr.* **2004**, *1037*, 283–298.
[35] S. Espinosa, E. Bosch, M. Rosés, *J. Chromatogr.* **2002**, *964*, 55–66.
[36] F. A. Cotton, R. Poli, *Inorg. Chem.* **1987**, *26*, 590–595.
[37] T. Ren, C. Lin, E. J. Valente, J. D. Zubkowski, *Inorg. Chim. Acta* **2000**, *297*, 283–290.
[38] L. G. Marzilli in *Advances in Inorganic Biochemistry, Metal Ions in Genetic Information Transfer, Vol. 3*, (Eds.: G. L. Eichhorn, L. G. Marzilli), Elsevier, North Holland, New York, **1981**, pp. 47–82.
[39] L. G. Marzilli, B. de Castro, C. Solorzano, *J. Am. Chem. Soc.* **1982**, *104*, 461–466, and references therein.
[40] D. W. Abbott, C. Woods, *Inorg. Chem.* **1983**, *22*, 1918–1924.
[41] E. Buncel, A. R. Norris, W. J. Racz, S. E. Taylor, *Inorg. Chem.* **1981**, *20*, 98–103.
[42] G. Barbarella, A. Bertoluzza, M. A. Morelli, M. R. Tosi, V. Tugnoli, *Gazz. Chim. Ital.* **1988**, *118*, 637–642.
[43] X. Jia, G. Zon, L. G. Marzilli, *Inorg. Chem.* **1991**, *30*, 228–239.
[44] S. Mukundan, Y. Xu, G. Zon, L. G. Marzilli, *J. Am. Chem. Soc.* **1991**, *113*, 3021–3027, and references therein.
[45] L. G. Marzilli, J. S. Saad, Z. Kuklenyik, K. A. Keating, Y. Xu, *J. Am. Chem. Soc.* **2001**, *123*, 2764–2770.
[46] Y. Qu, M. J. Bloemink, J. Reedijk, T. W. Hambley, N. Farrell, *J. Am. Chem. Soc.* **1996**, *118*, 9307–9313.
[47] L. J. Rinkel, C. Altona, *J. Biomol. Struct. Dyn.* **1987**, *5*, 621–649.
[48] D. G. Gorenstein, *in Phosphorus-31 NMR*; (Ed.: D. G. Gorenstein), Academic, New York, **1984**.
[49] C. Spellmeyer Fouts, L. G. Marzilli, R. A. Byrd, M. F. Summers, G. Zon, K. Shinozuka, *Inorg. Chem.* **1988**, *27*, 366–376.
[50] V. Beljanski, J. M. Villanueva, P. W. Doetsch, G. Natile, L. G. Marzilli, *J. Am. Chem. Soc.* **2005**, *127*, 15833–15842.
[51] T. R. Webb, J. D. Pollard, G. W. Goodloe, M. L. McKee, *Inorg. Chim. Acta* **1995**, *229*, 127–133.
[52] S. Teletchéa, S. Komeda, J.-M. Teuben, M.-A. Elizondo-Riojas, J. Reedijk, J. Kozelka, *Chem. Eur. J.* **2006**, *12*, 3741–3753.
[53] W. Saenger, *Principles of Nucleic Acid Structure*, Springer, **1984**, p. 61.
[54] M. Remin, *J. Biomol. Struct. Dyn.* **1997**, *15*, 251–264.
[55] B. Lippert, *Prog. Inorg. Chem.* **2005**, *54*, 385–447.
[56] M. Roitzsch, M. Garijo Añorbe, P. J. Sanz Miguel, B. Müller, B. Lippert, *J. Biol. Inorg. Chem.* **2005**, *10*, 800–812.
[57] S. L. Patt, J. N. Shoolery, *J. Magn. Reson.* **1982**, *46*, 535–539.
[58] C. Lecocq, J.-Y. Lallemand, *J. Chem. Soc. Chem. Commun.* **1981**, 150–152.
[59] F. Delaglio, S. Grzesiek, G. W. Vuister, G. Zhu, J. Pfeifer, A. Bax, *J. Biomol. NMR* **1995**, *6*, 277–293.
[60] A. K. Rappé, C. J. Casewit, K. S. Colwell, W. A. Goddard III, W. M. Skiff, *J. Am. Chem. Soc.* **1992**, *114*, 10024–10035.
[61] L. A. Castonguay, A. K. Rappé, *J. Am. Chem. Soc.* **1992**, *114*, 5832–5842.
[62] A. K. Rappé, K. S. Colwell, C. J. Casewit, *Inorg. Chem.* **1993**, *32*, 3438–3450.

Received: March 21, 2006
Published online: August 10, 2006

